



Sliding wear characteristics of solid lubricant coating on titanium alloy surface modified by laser texturing and ternary hard coatings

M. PREMANANTH, R. RAMESH

Department of Mechanical Engineering, Sri Venkateswara College of Engineering,
Sriperumbudur, Chennai-602117, Tamilnadu, India

Received 22 March 2016; accepted 28 June 2016

Abstract: Titanium alloys are poor in wear resistance and it is not suitable under sliding conditions even with lubrication because of its severe adhesive wear tendency. The surface modifications through texturing and surface coating were used to enhance the surface properties of the titanium alloy substrate. Hard and wear resistant coatings such as TiAlN and AlCrN were applied over textured titanium alloy surfaces with chromium as interlayer. To improve the friction and wear resisting performance of hard coatings further, solid lubricant, molybdenum disulphide (MoS₂), was deposited on dimples made over hard coatings. Unidirectional sliding wear tests were performed with pin on disc contact geometry, to evaluate the tribological performance of coated substrates. The tests were performed under three different normal loads for a period of 40 min at sliding velocity of 2 m/s. The tribological behaviours of multi-layer coatings such as coating structure, friction coefficient and specific wear rate were investigated and analyzed. The lower friction coefficient of approximately 0.1 was found at the early sliding stage, which reduces the material transfer and increases the wear life. Although, the friction coefficient increased to high values after MoS₂ coating was partially removed, substrate was still protected against wear by underlying hard composite layer.

Key words: surface texturing; chromium interlayer; hard coating; molybdenum disulphide; dry sliding

1 Introduction

The attractive properties such as lower modulus, superior biocompatibility and better corrosion resistance possessed by Ti–6Al–4V, $\alpha+\beta$ alloy, lead to its higher usage in structural and automobile field. More than 50% of all titanium alloys in use today are of this composition [1]. Ti–6Al–4V presently is the most widely used, high-strength titanium alloy. It finds a large application in aerospace, automotive, marine and chemical industries. Many research papers focused on the tribological improvement of titanium alloy surfaces only through the surface treatments and surface coatings [2–7]. The surface is the most important part of any engineering component. It is well known that most of the components fail from surface initiated defects such as wear, corrosion, fatigue or fracture. There is a constant demand for surfaces with improved tribological performance. Surface engineering, as opposed to bulk alloying, provides an opportunity to improve the wear resistance of engineering materials while leaving the

bulk characteristics relatively unchanged. The substrate material can be designed for strength and toughness while the coating is responsible for the resistance to wear, corrosion and thermal loads, and the achievement of the required frictional characteristics [8].

Surface texturing involves modifications of surface topography by creating an identical micro-relief with commonly shaped asperities or dimples. It helps to improve adhesion of the coating and to enhance the tribological properties of substrate materials. Among the various texturing techniques, laser surface texturing is one of the emerging techniques, which involves fabrication of artificial, regularly patterned micro-dimples over the substrate surface by a material ablation process with a pulsating laser beam, and thus it was employed to pattern substrate surfaces [9,10]. The use of surface coatings opens up the possibility for a material design in which the specific properties are located where they are most needed.

TiN and CrN are the most extensively investigated hard coatings due to their ability to provide high wear and corrosion resistance. The tribological performance of

TiN and CrN coatings can be improved by the addition of a third element such as Al, thus forming the TiAlN and AlCrN phases. Addition of aluminum results in the formation of oxides, which is very stable and prevents any form of erosion to the inner layers of these compounds and improves the elastic modulus, nano hardness and anti spalling of the coating [11]. The use of multi-layers has often been cited as the way forward to improve the mechanical, tribological and chemical properties of coatings. The metallic chromium interlayer can effectively improve the interface adhesion, wear resistance and reduce friction of hard coatings on soft substrates [12].

The surface modifications through texturing and surface coating were used to enhance the surface properties of the titanium alloy substrate. Further, to improve the friction and wear resisting performance of hard coatings, solid lubricant molybdenum disulphide (MoS_2), was deposited on dimples made over hard coatings. The lamellar structure of MoS_2 reduced the coefficient of friction and the underlying hard coating can successfully increase the load supporting capacity and improve the wear resistance [12–14]. The present investigation deals with the wear improvement of titanium-based alloy through surface modification by texturing followed by coating. The deposition of friction reduction coating on laser textured hard coating surfaces is a unique diversification in the current sliding wear analysis for effective wear resisting performance. This will meet the functional requirement of titanium alloy used in structural and automotive applications.

2 Experimental

2.1 Substrate material preparation and laser surface texturing

Mild annealed Ti–6Al–4V was chosen as the substrate material, which consists of 3.5%–4.5% V, 5.5%–6.75% Al, 0.4% Fe, 0.1% C (mass fraction), and balance titanium. Titanium alloy flats and cylindrical pins were procured from Noble Engineering Private Limited, Chennai, India, and machined to suitable sizes for tribological testing. Cylindrical pins made from mild annealed Ti–6Al–4V were first machined to a uniform diameter of 8 mm for a length of 40 mm. Further, the diameter of one end of the specimen was reduced to (4 ± 0.05) mm for a length of (5 ± 0.05) mm and preferred as the target end for the pin on disc experiment. Figure 1 shows the schematic diagram of the stepped cylindrical pin made from Ti–6Al–4V alloy.

The pin and flat specimens were mechanically polished by 1200 and 2000 mesh grit abrasive paper followed by polishing with 3 μm diamond paste. The

polished specimens with a final surface roughness of the order of 0.05–0.07 μm were cleaned ultrasonically in acetone to remove the burr and surface contaminants. Surface texturing was done on the polished specimens by using a commercial pulse Nd:YAG[®] laser beam. Among the various texturing techniques, laser surface texturing, which is one of the emerging techniques, involves fabrication of artificial, regularly patterned micro-dimples over the substrate surface by a material ablation process with a pulsating laser beam, and thus it was exploited to pattern titanium alloy surfaces. The surface texturing with laser beam is extremely fast, which requires short processing time and environment friendly. This provides excellent control of shape and size of the micro dimples, which allows realization of optimum designs. The laser beam operating parameters were 1.5 kHz pulsating beam, 1064 nm wavelength with a power of 11 kW and engraving speed of 50 mm/s. The texturing pattern was rectangular array and its schematic diagram is shown in Fig. 2.

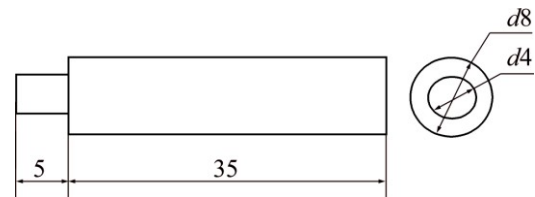


Fig. 1 Schematic diagram of cylindrical specimen used in pin on disc experiment (unit: mm)

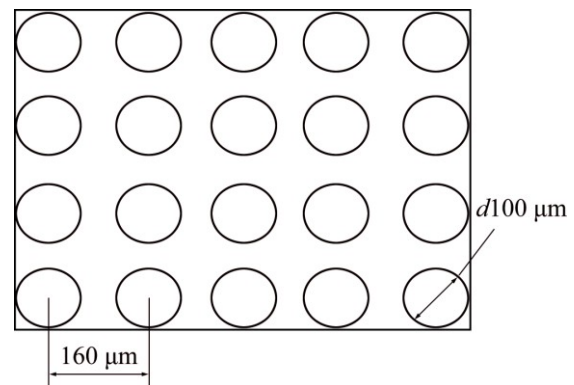


Fig. 2 Schematic diagram of rectangular array texturing pattern

The laser texturing was carried out over the target end surface for the following specifications based on the earlier research in Ref. [9]. The surface was processed to attain the texturing pattern as dimple density of 35%–45%, dimple diameter of 100–110 μm , dimple depth of 2.25–2.75 μm and distance between dimples of 150–160 μm . Figure 3(a) confirms the dimple arrangement and its dimensions on the polished titanium alloy surface. The close up view at the single dimple region clearly reveals the geometry of the dimple (Fig. 3 (b)).

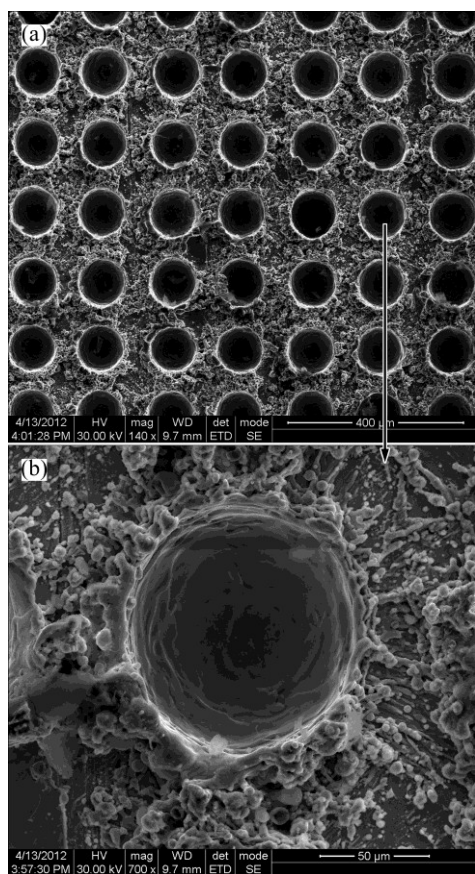


Fig. 3 Micrographs of laser textured surface of Ti-6Al-4V targeted for dimple density 40% and 100 μm diameter (a) and close up view at single dimple region confirming dimple geometry (b)

2.2 Surface coatings by physical vapour deposition (PVD)

Prior to the titanium aluminum nitride (TiAlN) and aluminum chromium nitride (AlCrN) coating, a chromium interlayer was deposited by DC magnetron sputtering technique. A 0.5–1.0 μm -thick interlayer was deposited by sputtering a chromium metal target mounted on one of the magnetrons. A substrate bias of -110 V , an arc current of 80 A and an argon pressure of 0.25 Pa were used during this deposition.

Cathodic arc evaporation physical vapour deposition technique was chosen for the deposition of ternary composite coatings such as TiAlN and AlCrN. The coating deposition time was 150 and 310 min for AlCrN and TiAlN coatings, respectively. The cathodic arc evaporation technique can be easily carried out in reactive gases like oxygen, nitrogen and hydrocarbons without any difficulty in controlling of the reactive gases and composite targets can be employed, which provide easy access to ternary compound. Arc vaporization provides a higher vaporization rate than sputtering. The cathodic arc deposition technique can be used to obtain very adherent and dense films and is the most widely

used arc technique when vaporizing alloy electrodes such as Ti and Al. In addition, the production cost of reactive arc evaporation is lower as compared to sputtering [15].

2.3 Surface preparation for solid lubricant coating

To improve the friction and wear resisting performance of the hard coatings further, the functionally graded solid lubricant coating, molybdenum disulphide (MoS_2) was deposited on it by spraying technique. The best performed coating surfaces such as AlCrN on textured surface with chromium interlayer in unidirectional sliding and TiAlN on textured surface with chromium interlayer in bidirectional sliding was selected for the MoS_2 deposition. The micro reservoirs were machined by Nd:YAG[®] laser beam on the hard coated surfaces and then reservoirs were filled by MoS_2 solid lubricant coating.

The deposition of solid lubricant coatings directly on the light metal substrates did not significantly improve the tribological properties, because of the low load bearing capacity of the substrate and poor adhesion of the coating [16]. The hard coatings with chromium interlayer on textured surfaces were preferred for MoS_2 coating, due to their better performance [17]. The micro reservoirs were machined by Nd:YAG[®] laser beam on the textured and coated surfaces with chromium interlayer. The reservoirs were filled by MoS_2 solid lubricant coating. The SEM image as shown in Fig. 4 shows the texturing pattern on the AlCrN coating surface by laser beam.

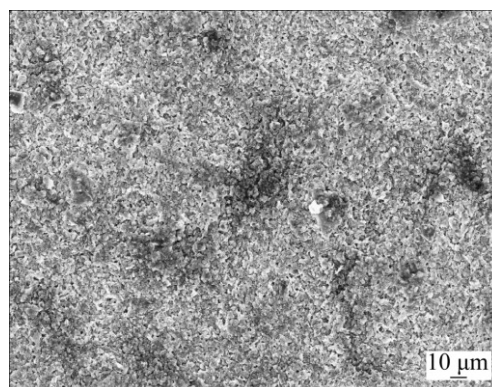


Fig. 4 SEM image of laser textured AlCrN coated surface

Strong adherent MoS_2 films can be produced by the use of bonding agents. The specimens were degreased with acetone and dried in air to remove the surface contaminants, followed by heating at $80\text{ }^\circ\text{C}$ for removing moisture. The fine MoS_2 particles with size of 0.5 to 1.0 μm were homogeneously dispersed in adhesive of resin system, which contained binder (novolac epoxy resin), solvent, and modifying agent. The mixture was sprayed onto the sample surfaces by a spray gun with

0.2 MPa nitrogen gas and cured in a container with relative humidity of 50%–55% and temperature of 30–35 °C. After solvent evaporation, a thin film was obtained on the substrate and then cured at 150 °C for 30 min followed by 180 °C for 60 min. The coated specimens were cooled in air and the loose MoS₂ powder on the surface was removed by soft brush [18,19].

2.4 Characterization of solid lubricant coating

The novolac epoxy resin-bonded solid lubricants deposited over the laser textured AlCrN surfaces was observed, as shown in Fig. 5. It shows that the coating was uniform with very dense deposition [19,20].

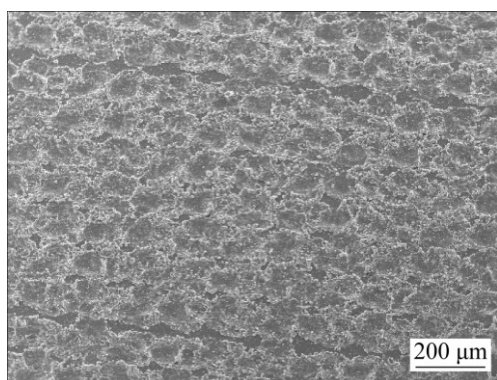


Fig. 5 Surface SEM image of MoS₂ solid lubricant coating deposited on laser textured AlCrN coating

A cross-sectional view of the specimen with coating is shown in Fig. 6. The SEM image shows the uniform distribution of the coating on the titanium alloy substrate. The range of thickness of the MoS₂ coating along with TiAlN and chromium interlayer was 14–15 μm. The chemical composition of the MoS₂ coating, analyzed by EDX, as shown in Fig. 7, confirms the presence of Mo (69.8%) as the main composition along with 14.5% S, 7.9% O and 7.8% C.



Fig. 6 SEM image on cross section of MoS₂-coated surface along with TiAlN composite coating and chromium as interlayer

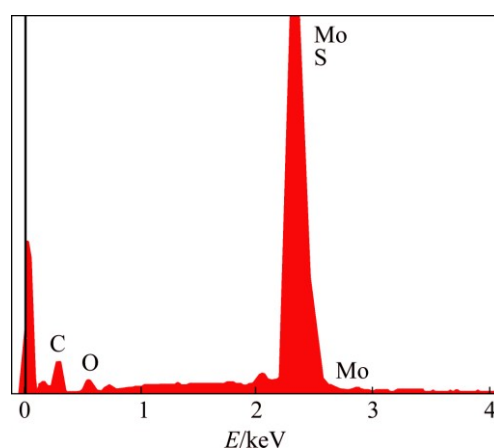


Fig. 7 EDX spectrum of MoS₂ coating

To analyze the coating structure, HRXRD (PANalytical X'Pert Pro MRD) with a Cu-target as X-ray source with a four crystal Ge (220) monochromator in the incident beam optics was used. The XRD pattern was recorded using Cu K_α radiation ($\alpha=1.5406 \text{ \AA}$) generated at 45 kV and 30 mA, scans were performed with a 2θ range of 0°–50° with 0.0197° step at a scan speed of 300 s/step. The XRD pattern presented in Fig. 8, shows the diffraction peaks corresponding to (0 0 2), (0 0 4), (1 0 0), (1 0 2), (1 0 3), (0 0 6), (1 0 5), and (1 1 0) planes which confirmed that the MoS₂ solid lubricant coating was prepared successfully. All diffraction peaks belonging to MoS₂ can be indexed to hexagonal close packed structure. These findings are accordance with the experimental results published in Ref. [18].

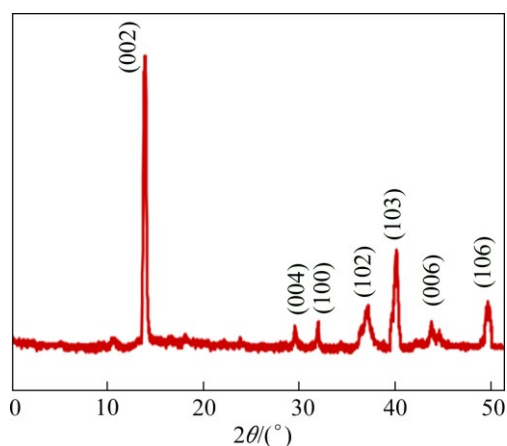


Fig. 8 XRD pattern of MoS₂ solid lubricant coating

2.5 Unidirectional sliding wear behaviour by pin on disc tribometer

As outlined by ASTM G99–04, pin-on-disk testing consists of a rotating disk in contact with a stationary cylindrical pin along with an applied normal load at the top. The schematic diagram of a pin on disc wear testing working principle is shown in Fig. 9.

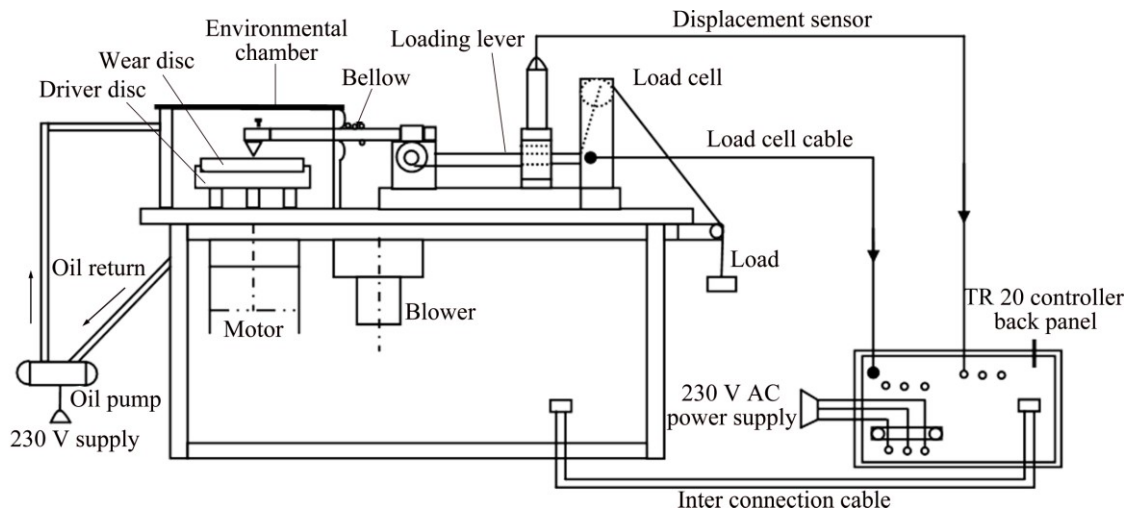


Fig. 9 Schematic diagram of pin on disc tribometer

The rotary wear friction test reproduces the rotational motion found in many real-world tribology mechanisms. A stationary, precisely known mass cylindrical pin (specimen) is loaded onto a rotating disc (counterbody) at a specific position from the center of rotation. As the disc starts rotating, the pin tip creates a rotational wear track. Friction force was accurately measured during the test by a load cell contacting with the cantilever arm in the machine. Friction coefficient was calculated from the friction force with known normal load applied. Wear rates for the pin and the sample are calculated from the volume of material lost during the test. A wide variety of testing is possible by varying sliding radius, normal load and sliding speed during the test. The tribological properties such as, friction coefficient, wear volume, wear rate and wear mechanisms can be analyzed through this instrument. The wear tests were carried out as per ASTM standard G 99 under dry sliding contact conditions at room temperature and the total testing time was about 40 min.

Continuous sliding of surfaces leads to increase in the wear rate of the pins. The mass of the pin before and after the test was measured using a precision electronic mass balance instrument. Wear loss represented as specific wear rate (k) was quantified from Eq. (1):

$$k = \frac{m_1 - m_2}{\rho F_n s} \quad (1)$$

where k is the specific wear rate in $\text{mm}^3/(\text{N}\cdot\text{m})$, ρ is the density of the material in kg/mm^3 , m_1 and m_2 are the initial and final masses of pin in g, F_n is the applied normal load in N and s is the total sliding distance in m.

3 Results and discussion

The coefficient of friction at different normal loads as a function of sliding distance is shown in Figs. 10 and

11. The low coefficient of friction of approximately 0.1 was found at the early sliding stage. Early increase in friction coefficient was observed at higher normal loads and this behaviour confirms that coating resistance against sliding wear reduced as the normal load

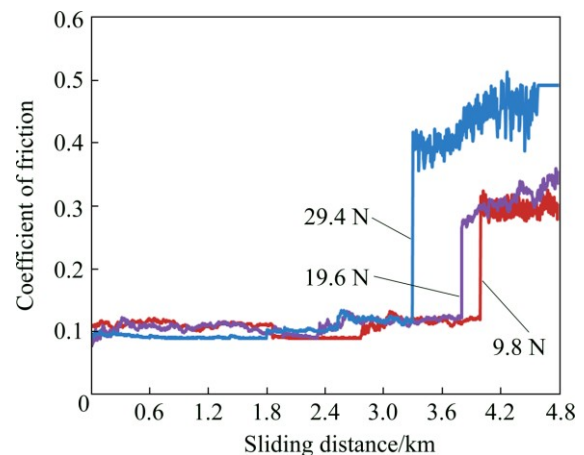


Fig. 10 Friction coefficient of MoS_2 coating on textured TiAlN coated surfaces as function of sliding distance

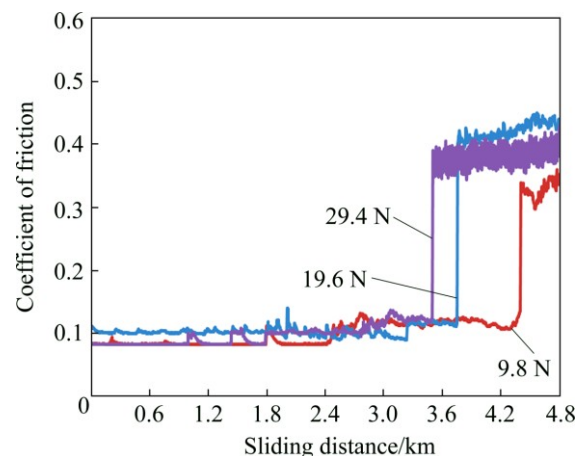


Fig. 11 Friction coefficient of MoS_2 coating on textured AlCrN coated surfaces as function of sliding distance

increased. The results corroborate with the findings in the research study in Ref. [18].

The average coefficient of friction was 0.32 for TiAlN coatings without chromium interlayer, 0.30 for the coatings with chromium interlayer and 0.20 for the MoS₂-coated surfaces. The average coefficient of friction was 0.31 for AlCrN coatings without Cr as interlayer, 0.29 for the coatings with chromium interlayer and 0.19 for the MoS₂-coated surfaces. Lower coefficient of friction reduces the material transfer and increases the wear life [18]. Although the friction coefficient increased to high coefficient of friction after the MoS₂ coating was partially removed from the contact region, the titanium alloy substrate was still protected against wear by the hard composite layer.

The deposition of a MoS₂ layer on the top of composite multi-layered coating has a beneficial effect on the wear resistance of the coated samples. The total sliding distances of MoS₂ coating on hard coatings are compared in Table 1 under different normal loads applied. Among the samples tested, MoS₂ coating on textured AlCrN had the highest sliding distance at all normal loads. The highest sliding distance of 4.40 km was observed at 9.8 N normal load. It was 27% higher than the AlCrN coating on textured surfaces with Cr interlayer and 38% higher than the same coating without Cr as interlayer. The reason for increased sliding distance was that the MoS₂ coating on textured surface reduced the friction coefficient between coating and counterbody and because of its improved adhesive bonding with AlCrN coating.

Table 1 Comparison of total sliding distance between MoS₂-coated TiAlN and AlCrN coating

Normal load/N	Sliding distance/km	
	Cr-TiAlN-MoS ₂	Cr-AlCrN-MoS ₂
9.8	4.00	4.40
19.6	3.30	3.75
29.4	3.00	3.50

The specific wear rate of MoS₂ solid lubricant coating on TiAlN and AlCrN hard coatings is compared in Fig. 12. The wear rate of MoS₂ on TiAlN was higher as compared to the MoS₂ on AlCrN coating. The wear rate was reduced by at least one order of magnitude with a top layer of MoS₂ when compared with that for a hard composite coating without MoS₂. The MoS₂ film is removed during sliding and constituted a source of lubricating particles that adhere to both the contacting bodies and limit the mating of the surfaces, which increased the wear life.

The specific wear rate was reduced by at least one order of magnitude with a top layer of MoS₂ when compared with that of a hard composite coating without

MoS₂. The appreciable wear resisting performance was observed by MoS₂ deposition. The lowest wear rate of about $1.2564 \times 10^{-8} \text{ mm}^3/(\text{N}\cdot\text{m})$ was observed on textured Cr-AlCrN-MoS₂ coating at 9.8 N normal load.

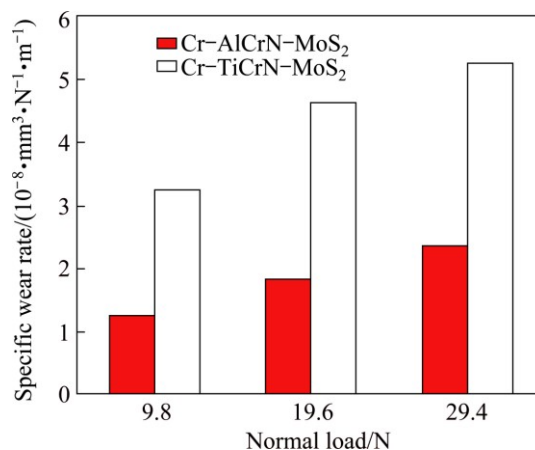


Fig. 12 Specific wear rate vs normal load of solid lubricant MoS₂ coating deposited on hard TiAlN and AlCrN coatings under unidirectional sliding

4 Wear morphology analysis

The optical micrographs of the worn out pin surfaces are shown in Fig. 13. The surface of MoS₂-coated AlCrN was smoother than the TiAlN surface. The addition of solid lubricant film improved the dry friction behavior significantly. Although the solid lubricant coating worn out gradually, it existed at the contact region as well as boundary of the wear scar, which prevented the direct contact of counterbody with underlying hard coating and substrate. Thus, the friction coefficient was reduced and thereby the wear life was increased.

The morphology of textured worn out pin surface was observed by SEM and its micrograph is shown in Fig. 14. Unlike the hard coated textured surfaces either with or without interlayer, almost all the dimples were filled with the coating composition and also the surface was smooth and free from any loose wear debris. Further, the EDX analysis was performed at the dimple region marked in Fig. 14.

The EDX analysis result as shown in Fig. 15, confirms the presence of solid lubricant particles and its binding material as the major composition. Ti peaks were also observed, which confirm the partial exposure of underlying TiAlN hard coating after the wear test. MoS₂ solid lubricant possesses extremely low friction and easy shearing property. As a result it did not wear out counterbody material during sliding. This can be cited as the reason for no trace of iron in the EDX spectrum analysis.

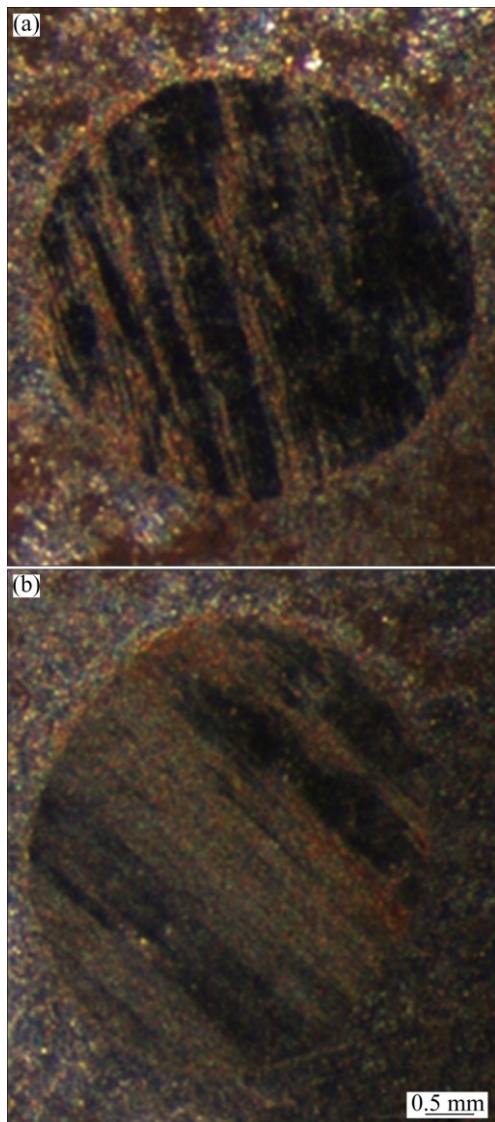


Fig. 13 Optical micrographs of MoS₂-coated worn pin surfaces of textured TiAlN coating (a) and textured AlCrN coating (b) after wear test against AISI52100 disc at 29.4 N

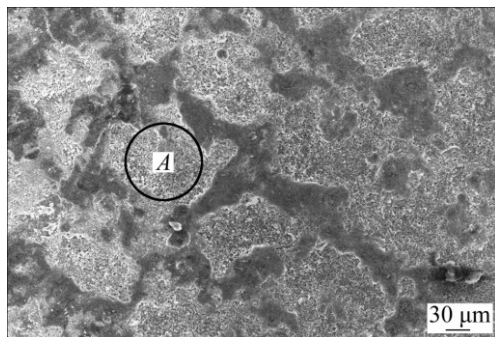


Fig. 14 SEM image of TiAlN coating on textured specimen after wear at 29.4 N

4.1 Wear debris analysis collected from MoS₂ coating deposited on AlCrN and TiAlN hard coatings

The majority of particles observed by SEM (Fig. 16) are in fact agglomerates constituted by far smaller

particles which then disperse during sliding. The deposition of MoS₂ layer on top of composite multi-layered coating had a beneficial effect on the wear resistance of the coated-samples. Extremely low wear rates and the intrinsic property of MoS₂ as easy shearing are likely to produce very small wear particles.

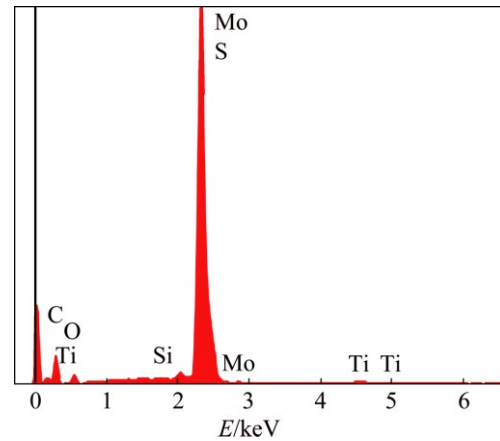


Fig. 15 EDX spectrum of TiAlN coating on textured specimen after wear at 29.4 N

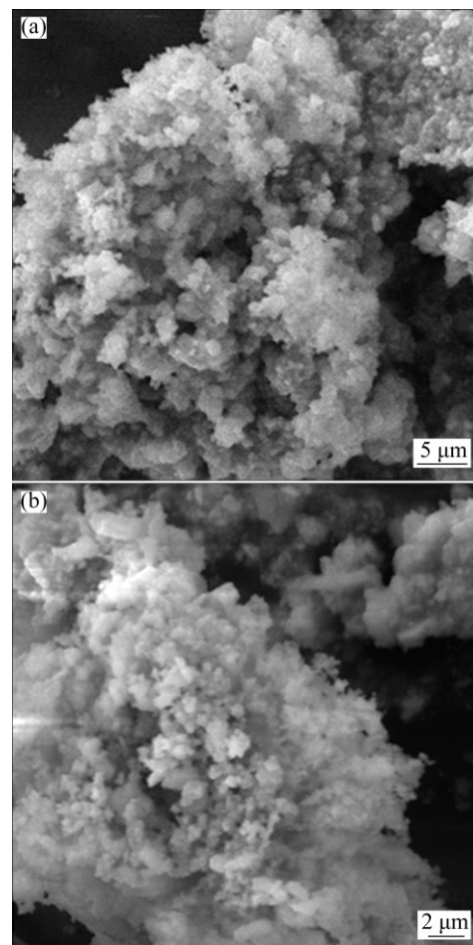


Fig. 16 SEM images of wear debris collected from MoS₂ coating on AlCrN coating (a) and TiAlN coating (b) tested at 29.4 N

Tiny wear debris was observed by SEM which is essential for the increased wear life of the component being coated. The MoS₂ film is removed during sliding and constitutes a source of lubricating particles that adhere itself and also on the contacting bodies which could reduce the mating of the surfaces. The limited surface contact reduces the friction coefficient and increases the wear life.

4.2 Mechanism of wear

Figure 17 explains the sequence of deposition of MoS₂ solid lubricant coatings over the textured hard coating surface. The dimples on the substrate are partially filled during chromium deposition. The remaining portion is filled during the AlCrN or TiAlN composite coating. This led to better integrity and enhanced adhesion ability, which promoted chemical affinity and mechanical interlocking of the coatings with substrate.

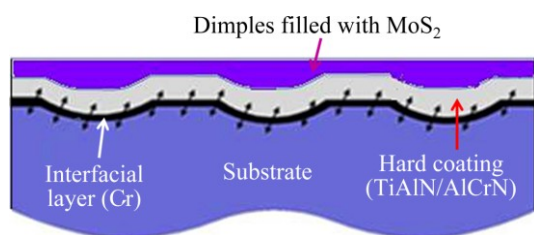


Fig. 17 Schematic diagram of coating cross section for textured substrate modified with MoS₂ coating deposited on hard coating dimples

Again, the micro reservoirs were machined by laser beam on the hard coated surfaces and then reservoirs were filled by MoS₂ solid lubricant coating. Additional mechanical locking was provided to MoS₂ coating. This surface design resisted wear more effectively and retained large amount of coating at the contact region under shear traction. The lowest friction coefficient possessed by the top layer along with the artificially provided mechanical locking, reduced the material transfer and increased the wear life. Even after the solid lubricant coating was consumed, the PVD-coated composite coating provides wear protection for the metal substrate.

During sliding, release of MoS₂ debris and subsequently released hard composite wear particles in combination led to low friction characteristics between the contacting surfaces and resulted in improved wear resisting performance. The stored solid lubricant coating in the dimples and its release during sliding motion, load bearing support provided by the underlying hard coating and increased bonding strength of the hard coating with substrate through surface texturing and chromium interlayer, worked together to increase the coating

performance. The above findings are in accordance with the experimental results reported by BASNYAT et al [21].

5 Conclusions

1) The hexagonal crystal structure with the intrinsic property of easy shearing possessed by MoS₂ reduced the friction coefficient between contact surfaces. The lowest friction coefficient of top layer MoS₂, reducing the material transfer at the contact region, has increased the wear life for a large number of cycles. Although the coefficient of friction increased to high values when MoS₂ coating was removed during sliding, the light metal substrate was still protected against seizing by the underlying PVD deposited composite coating.

2) The highest sliding distance of 4.40 km and the lowest wear rate of $1.2564 \times 10^{-8} \text{ mm}^3/(\text{N}\cdot\text{m})$ were observed for the MoS₂-coating applied over the textured AlCrN coating tested at 9.8 N normal load under unidirectional sliding motion. During sliding, release of MoS₂ and subsequently released hard composite wear particles in combination leads to low friction characteristics between the contacting surfaces and resulted in improved wear resisting performance.

3) In addition to the reduced friction coefficient offered by solid lubricant coating, the load bearing support provided by the underlying hard coating and increased bonding strength of the hard coating with substrate through surface texturing and chromium interlayer, worked together to increase the coating performance.

References

- [1] LEYENS C, PETERS M. Titanium and titanium alloys [M]. Germany: WILEY-VCH Verlag GmbH & Cos, 2003.
- [2] DONG H, BELL T. Enhanced wear resistance of titanium surfaces by a new thermal oxidation treatment [J]. *Wear*, 1999, 238: 131–137.
- [3] WU L L, HOLLOWAY B C, PRASAD BEESABATHINA D, KALIL C, MANOS D M. Analysis of diamond-like carbon and Ti/MoS₂ coatings on Ti–6Al–4V substrates for applicability to turbine engine applications [J]. *Surface & Coatings Technology*, 2000, 130: 207–217.
- [4] BUDZYNSKI P, YOUSSEF A A, SIELANKO J. Surface modification of Ti–6Al–4V alloy by nitrogen ion implantation [J]. *Wear*, 2006, 261: 1271–1276.
- [5] LEE C, SANDERS A, TIKEKAR N, CHANDRAN K S R. Tribology of titanium boride-coated titanium balls against alumina ceramic: Wear, friction, and micromechanisms [J]. *Wear*, 2008, 265: 375–386.
- [6] COSTA M Y P, CIOFFI M O H, VOORWALD H J C, GUIMARAES V A. An investigation on sliding wear behavior of PVD coatings [J]. *Tribology International*, 2010, 43: 2196–2202.
- [7] MARTINI C, CESCHINI L, CASADEI B, BOROMEI I, GUION J B. Dry sliding behaviour of hydrogenated amorphous carbon (a-C:H) on Ti–6Al–4V coatings [J]. *Wear*, 2011, 271: 2025–2036.
- [8] BALOYI N M, POPOOLA A P I, PITYANA S L. Microstructure, hardness and corrosion properties of laser processed Ti6Al4V-based

- composites [J]. Transactions of Nonferrous Metals Society of China, 2015, 25: 2912–2923.
- [9] RAPOPORT L, MOSHKOVICH A, PERFILYEV V, LAPSKER I, HALPERIN G, ITOVICH Y, ETSION I. Friction and wear of MoS₂ films on laser textured steel surfaces [J]. Surface & Coatings Technology, 2008, 202: 3332–3340.
- [10] HU T, HU L. Tribological properties of lubricating films on the Al–Si alloy surface via laser surface texturing [J]. Tribology Transactions, 2011, 54: 800–805.
- [11] MO J L, ZHUA M H, LEIA B, LENG Y X, HUANG N. Comparison of tribological behaviours of AlCrN and TiAlN coatings deposited by physical vapor deposition [J]. Wear, 2007, 263: 1423–1429.
- [12] THEILER G, GRADT T, OSTERLE W, BRUCKNER A, WEIHNACHT V. Friction and endurance of MoS₂/ta-C coatings produced by laser arc deposition [J]. Wear, 2013, 297: 791–801.
- [13] TANG Gang, HUANG Wang-juan, CHANG Dao-fang, NIE Wen-zhong, MI Wei-jian, YAN Wei. The friction and wear of aramid fiber-reinforced polyamide 6 composites filled with nano-MoS₂ [J]. Polymer-Plastics Technology and Engineering, 2011, 50: 1537–1540.
- [14] ZHANG W Y, DEMYDOV D, JAHAN M P, MISTRY K, ERDEMIR A, MALSHE A P. Fundamental understanding of the tribological and thermal behavior of Ag–MoS₂ nano particle-based multi-component lubricating system [J]. Wear, 2012, 288: 9–16.
- [15] SEIBERT F, DOBELI M, FOPP-SPORI D M. Comparison of arc evaporated Mo-based coatings versus Cr₁N₁ and Ta–C coatings by reciprocating wear test [J]. Wear, 2013, 298–299: 14–22.
- [16] SEITZMAN L E, BOLSTER R N, SINGER I L. IBAD MoS₂ lubrication of titanium alloys [J]. Surface & Coatings Technology, 1996, 78(1–3): 10–13.
- [17] ANANTH M P, RAMESH R. Reciprocating sliding wear performance of hard coating on modified titanium alloy surfaces [J]. Tribology Transactions, 2015, 58: 169–176.
- [18] XU J, ZHU M H, ZHOU Z R, KAPSA P H, VINCENT L. An investigation on fretting wear life of bonded MoS₂ solid lubricant coatings in complex conditions [J]. Wear, 2003, 255: 253–258.
- [19] LUO J, ZHU M H, WANG Y D, ZHENG J F, MO J L. Study on rotational fretting wear of bonded MoS₂ solid lubricant coating prepared on medium carbon steel [J]. Tribology International, 2011, 44: 1565–1570.
- [20] YE Yin-ping, CHEN Jian-min, ZHOU Hui-di. An investigation of friction and wear performances of bonded molybdenum disulfide solid film lubricants in fretting conditions [J]. Wear, 2009, 266: 859–864.
- [21] BASNYAT P, LUSTER B, MURATORE C, VOEVODIN A A, HAASCH R, ZAKERI R, KOHLI P, AOUADI S M. Surface texturing for adaptive solid lubrication [J]. Surface & Coatings Technology, 2008, 203: 73–79.

激光处理钛合金表面和三元硬质 涂层表面固体润滑涂层的滑动磨损特性

M. PREM ANANTH, R. RAMESH

Department of Mechanical Engineering, Sri Venkateswara College of Engineering,
Sriperumbudur, Chennai-602117, Tamilnadu, India

摘要: 钛合金的耐磨度较差, 因其严重的粘着磨损倾向, 不适合润滑滑动。通过织构化和表面涂层进行表面修饰, 以提高钛合金基体的表面性能。硬质和耐磨涂层如 TiAlN 和 AlCrN 被应用于钛合金表面, 以铬作为中间层。为了进一步提高硬质涂层的耐摩擦磨损性能, 使用固体润滑剂二硫化钼沉积在硬质涂层的微坑。采用销-盘实验对涂覆基材进行单向滑动磨损测试, 以评估其摩擦性能。在 3 个不同的载荷、时间 40 min、2 m/s 滑移速度下进行测试, 分析研究多层涂层的摩擦行为, 如涂层结构、摩擦因数和比磨损率。在滑移初期阶段, 摩擦因数较低, 约为 0.1, 这降低了材料转移, 延长了耐磨寿命。除去部分二硫化钼涂层后, 摩擦因数增大到较高值, 硬质复合层仍然保护基体以免磨损。

关键词: 表面织构化; 铬层; 硬质涂层; 二硫化钼; 干滑动

(Edited by Xiang-qun LI)